

---

---

# Imaging P-Glycoprotein Induction at the Blood–Brain Barrier of a $\beta$ -Amyloidosis Mouse Model with $^{11}\text{C}$ -Metoclopramide PET

Viktoria Zoufal<sup>1</sup>, Severin Mairinger<sup>1</sup>, Mirjam Brackhan<sup>2</sup>, Markus Krohn<sup>2</sup>, Thomas Filip<sup>1</sup>, Michael Sauberer<sup>1</sup>, Johann Stanek<sup>1</sup>, Thomas Wanek<sup>1</sup>, Nicolas Tournier<sup>3</sup>, Martin Bauer<sup>4</sup>, Jens Pahnke<sup>2,5–7</sup>, and Oliver Langer<sup>1,4,8</sup>

<sup>1</sup>Preclinical Molecular Imaging, AIT Austrian Institute of Technology GmbH, Seibersdorf, Austria; <sup>2</sup>Department of Neuro-/Pathology, University of Oslo and Oslo University Hospital, Oslo, Norway; <sup>3</sup>UMR 1023 IMIV, Service Hospitalier Frédéric Joliot, CEA, INSERM, Université Paris Sud, CNRS, Université Paris-Saclay, Orsay, France; <sup>4</sup>Department of Clinical Pharmacology, Medical University of Vienna, Vienna, Austria; <sup>5</sup>LIED, University of Lübeck, Lübeck, Germany; <sup>6</sup>Leibniz-Institute of Plant Biochemistry, Halle, Germany; <sup>7</sup>Department of Pharmacology, Medical Faculty, University of Latvia, Rīga, Latvia; and <sup>8</sup>Division of Nuclear Medicine, Department of Biomedical Imaging and Image-Guided Therapy, Medical University of Vienna, Vienna, Austria

P-glycoprotein (ABC subfamily B member 1, ABCB1) plays an important role at the blood–brain barrier (BBB) in promoting clearance of neurotoxic  $\beta$ -amyloid (A $\beta$ ) peptides from the brain into the blood. ABCB1 expression and activity were found to be decreased in the brains of Alzheimer disease patients. Treatment with drugs that induce cerebral ABCB1 activity may be a promising approach to delay the build-up of A $\beta$  deposits in the brain by enhancing clearance of A $\beta$  peptides from the brain. The aim of this study was to investigate whether PET with the weak ABCB1 substrate radiotracer  $^{11}\text{C}$ -metoclopramide can measure ABCB1 induction at the BBB in a  $\beta$ -amyloidosis mouse model (APP/PS1-21 mice) and in wild-type mice. **Methods:** Groups of wild-type and APP/PS1-21 mice aged 50 or 170 d underwent  $^{11}\text{C}$ -metoclopramide baseline PET scans or scans after intraperitoneal treatment with the rodent pregnane X receptor activator 5-pregnen-3 $\beta$ -ol-20-one-16 $\alpha$ -carbonitrile (PCN, 25 mg/kg) or its vehicle over 7 d. At the end of the PET scans, brains were harvested for immunohistochemical analysis of ABCB1 and A $\beta$  levels. In separate groups of mice, radiolabeled metabolites of  $^{11}\text{C}$ -metoclopramide were determined in plasma and brain at 15 min after radiotracer injection. As an outcome parameter of cerebral ABCB1 activity, the elimination slope of radioactivity washout from the brain ( $k_{E,\text{brain}}$ ) was calculated. **Results:** PCN treatment resulted in an increased clearance of radioactivity from the brain as reflected by significant increases in  $k_{E,\text{brain}}$  (from +26% to +54% relative to baseline). Immunohistochemical analysis confirmed ABCB1 induction in the brains of PCN-treated APP/PS1-21 mice with a concomitant decrease in A $\beta$  levels. There was a significant positive correlation between  $k_{E,\text{brain}}$  and ABCB1 levels in the brain. In wild-type mice, a significant age-related decrease in  $k_{E,\text{brain}}$  was found. Metabolite analysis showed that most radioactivity in the brain comprised unmetabolized  $^{11}\text{C}$ -metoclopramide in all animal groups. **Conclusion:**  $^{11}\text{C}$ -metoclopramide can measure ABCB1 induction in the mouse brain without the need to consider an arterial input function and may find potential application in Alzheimer disease patients to noninvasively evaluate strategies to enhance the clearance properties of the BBB.

**Key Words:** Alzheimer disease; APP/PS1-21 mice;  $\beta$ -amyloid clearance; P-glycoprotein induction;  $^{11}\text{C}$ -metoclopramide

**J Nucl Med 2020; 61:1050–1057**  
DOI: 10.2967/jnumed.119.237198

**A** common feature of age-related neurodegenerative diseases (e.g., Alzheimer disease [AD], Parkinson disease, frontotemporal dementia, Huntington disease, and amyotrophic lateral sclerosis) is the presence of misfolded and aggregated proteins that lose their physiologic roles and acquire neurotoxic properties (1). In these so-called proteinopathies, the accumulation of proteins in the brain has been linked to their insufficient clearance from the brain (1–3). Several different mechanisms for removal of neurotoxic proteins from the brain have been described, with extrusion into the circulation via the blood–brain barrier (BBB) being an important one (1). Transfer of substances across the BBB is tightly controlled. One important functional component of the BBB is adenosine triphosphate-binding cassette (ABC) transporters, which are expressed mainly in the luminal plasma membrane of brain capillary endothelial cells and which accept numerous endogenous and exogenous compounds as their substrates (4). An important representative of this family of transporters at the BBB is P-glycoprotein (ABC subfamily B member 1, ABCB1). ABCB1 was shown to work together with the low-density-lipoprotein-receptor-related protein 1 in the abluminal membrane of brain capillary endothelial cells in translocating  $\beta$ -amyloid (A $\beta$ ) peptides across the BBB (5). Several studies found a decrease in ABCB1 expression and activity in patients and mouse models of AD, which may contribute to a reduced A $\beta$  clearance across the BBB (6–10).

Treatment with drugs that induce ABCB1 activity at the BBB may be a promising approach to attenuate AD symptoms caused by cerebral A $\beta$  deposition by enhancing clearance of neurotoxic A $\beta$  peptides from the brain (1). Numerous signaling pathways that regulate cerebral ABC transporter expression are currently known (11). Agents targeting various components of these pathways have been tested in different  $\beta$ -amyloidosis mouse models for their ability to restore ABCB1 activity or expression in the brain and thereby

---

Received Sep. 25, 2019; revision accepted Nov. 18, 2019.  
For correspondence or reprints contact: Oliver Langer, Preclinical Molecular Imaging, AIT Austrian Institute of Technology GmbH, 2444 Seibersdorf, Austria.  
E-mail: oliver.langer@ait.ac.at  
Published online Dec. 5, 2019.  
COPYRIGHT © 2020 by the Society of Nuclear Medicine and Molecular Imaging.

decrease cerebral A $\beta$  load (9,12–14). A future translation of such therapeutic approaches to AD patients critically depends on the availability of a diagnostic tool to measure ABCB1 activity at the human BBB.

PET with radiolabeled ABCB1 substrates, such as (*R*)-<sup>11</sup>C-verapamil and <sup>11</sup>C-*N*-desmethyl-loperamide, has shown great promise to study the effects of ABCB1 inhibition at the BBB on brain penetration of ABCB1 substrates (15–17). However, currently available PET tracers are avid substrates of ABCB1 that possess very low brain uptake when ABCB1 is fully functional, limiting their applicability to study the effects of ABCB1 induction at the BBB (18,19). Consequently, weak substrates of ABCB1 have been developed for PET, such as <sup>11</sup>C-metoclopramide (20) or <sup>18</sup>F-MC225 (21). Translational PET studies on rats, nonhuman primates, and healthy human volunteers demonstrated that baseline brain uptake of <sup>11</sup>C-metoclopramide is substantially higher than that of (*R*)-<sup>11</sup>C-verapamil or <sup>11</sup>C-*N*-desmethyl-loperamide and significantly increased after ABCB1 inhibition with tariquidar or cyclosporine A (20,22,23).

In the present study, we assessed the suitability of <sup>11</sup>C-metoclopramide to measure ABCB1 induction at the BBB in a commonly used  $\beta$ -amyloidosis mouse model (APP/PS1-21 mice) (24) and in wild-type mice by using a validated ABCB1 induction protocol based on treatment with the prototypical rodent pregnane X receptor (PXR) activator 5-pregnen-3 $\beta$ -ol-20-one-16 $\alpha$ -carbonitrile (PCN) (9).

## MATERIALS AND METHODS

### Chemicals

Unless otherwise stated, all chemicals were purchased from Sigma-Aldrich or Merck. Metoclopramide ampules (Paspertin [Mylan Österreich GmbH, Vienna, Austria]; 10 mg/2 mL) were obtained from a local pharmacy. PCN was dissolved in safflower oil containing 5% (v/v) dimethyl sulfoxide and was injected intraperitoneally into mice at a dose of 25 mg/kg of body weight (9).

### Radiotracer Synthesis

<sup>11</sup>C-metoclopramide was synthesized as described before (25). For intravenous injection into animals, <sup>11</sup>C-metoclopramide was formulated in 0.9% (w/v) physiologic saline, and 10  $\mu$ L of metoclopramide solution (containing 0.05 mg of unlabeled metoclopramide) was added to each injected dose (to slow peripheral metabolism of the radiotracer) (20). Radiochemical purity was more than 98%.

### Animals

Female transgenic mice that express mutated human amyloid precursor protein (APP) and presenilin 1 (PS1) under control of the Thy1-promoter (APP<sub>KM670/671NL</sub>, PS<sub>L166P</sub>) (referred to as APP/PS1-21 mice) (24) and wild-type mice were maintained in a C57BL/6J genetic background at the University of Oslo. Two different age groups of wild-type mice were examined: approximately 50 d (mean age, 48  $\pm$  1 d; mean weight, 18.9  $\pm$  1.9 g) and approximately 170 d (mean age, 162  $\pm$  26 d; mean weight, 26.8  $\pm$  3.5 g). APP/PS1-21 mice were investigated at an approximate age of 50 d (mean age, 52  $\pm$  1 d; mean weight, 18.4  $\pm$  1.3 g) and 170 d (mean age, 168  $\pm$  20 d; mean weight, 24.6  $\pm$  2.3 g). In total, 65 mice were used in the experiments. The study was approved by the national authorities (Amt der Niederösterreichischen Landesregierung), and study procedures were in accordance with the European Communities Council Directive of September 22, 2010 (2010/63/EU). The animal experimental data reported in this study are in compliance with the ARRIVE (Animal Research: Reporting In Vivo Experiments) guidelines.

### Experimental Design

An overview of the examined animal groups is given in Table 1. Groups of wild-type and APP/PS1-21 mice underwent a baseline PET

**TABLE 1**  
Overview of Examined Animal Groups and Numbers

Group	PET		Metabolism (170 d old)
	50 d old	170 d old	
Wild-type baseline	5	10	0
Wild-type PCN	0	4*	1
Wild-type vehicle	0	3*	3
APP/PS1-21 baseline	8	6	0
APP/PS1-21 PCN	0	8	2
APP/PS1-21 vehicle	0	4*	4

\*Same animals also received baseline scan.

scan with <sup>11</sup>C-metoclopramide. After the baseline scan, animals were intraperitoneally treated for 7 d once daily with PCN (25 mg/kg) or with vehicle solution (5% dimethyl sulfoxide in safflower oil). In the case of APP/PS1-21 mice, a separate group of animals (that had not undergone baseline PET scans) was used for PCN treatment (to improve the tolerability of PCN treatment). On the day after the last treatment, the animals underwent a PET scan with <sup>11</sup>C-metoclopramide. The dose of PCN was based on previous work (9). Separate groups of vehicle- and PCN-treated animals were used to assess radiotracer metabolism.

### PET Imaging

Imaging experiments were performed under isoflurane/air anesthesia. The animals were warmed throughout the experiment, and body temperature and respiratory rate were constantly monitored. The mice were placed in a custom-made imaging chamber, and a lateral tail vein was cannulated. A microPET Focus220 scanner (Siemens Medical Solutions) was used for PET imaging. <sup>11</sup>C-metoclopramide (26  $\pm$  6 MBq in a volume of 100  $\mu$ L) was administered as an intravenous bolus over 60 s, and a 90-min dynamic PET scan was initiated at the start of radiotracer injection. List-mode data were acquired with a timing window of 6 ns and an energy window of 250–750 keV. After the 7-d treatment period, the mice underwent a 90-min dynamic <sup>11</sup>C-metoclopramide PET scan using the same acquisition parameters. At the end of the PET scan, a blood sample was collected from the retrobulbar plexus and the animals were killed by cervical dislocation. Blood was centrifuged to obtain plasma, and aliquots of blood and plasma were measured for radioactivity in a  $\gamma$ -counter. Whole brains were removed, incubated in 30% sucrose solution, and embedded in Tissue Freezing Medium (Tissue-Tek O.C.T Compound; Sakura Finetek). Samples were snap-frozen in liquid nitrogen and stored at  $-80^{\circ}\text{C}$  for immunohistochemistry of ABCB1 and A $\beta$ .

### Immunohistochemistry

Immunohistochemistry was performed as described before (6). After being defrosted from  $-80^{\circ}\text{C}$  to  $-20^{\circ}\text{C}$ , the brains were cut into transversal 10- $\mu$ m-thick slices with a cryostat (Microm HM 550; Thermo Fisher Scientific). Frozen sections of 3 brain regions—cortex, hippocampus, and cerebellum—were mounted on coated slides (VWR Superfrost Plus; VWR International) and stored at  $-80^{\circ}\text{C}$ . Later, the thawed brain slices were fixed either with 4% paraformaldehyde for ABCB1 staining or with methanol/acetone (1:1) for A $\beta$  staining. Afterward, the slides were unmasked with acetic acid/ethanol (1:3) at  $-20^{\circ}\text{C}$  for ABCB1

immunohistochemistry, washed in 0.1 M tris-buffered saline, and placed in endogenous peroxidase blocking solution consisting of 0.5% H<sub>2</sub>O<sub>2</sub> (v/v) for 30 min. The slides were then washed and inserted into cover plates (Thermo Scientific Shandon Glass Coverplates; Fisher Scientific) to achieve standardized staining results. To avoid nonspecific reactions, blocking solution was added for 1 h at room temperature. Brain slices were then incubated with the respective primary antibody (1:200, anti-ABCB1 antibody [EPR10364, recognizes both mouse ABCB1A and mouse ABCB1B; Abcam]; 1:300, anti-beta amyloid antibody [ab3539; Abcam]) or with antibody carrier solution for the negative control at 4°C overnight. On the next day, the slides were rinsed with tris-buffered saline and the secondary antibody (1:500, Biotin-SP [long spacer] [AffiniPure donkey anti-rabbit IgG (H+L); Jackson Immuno Research]) was applied at room temperature for 60 min. After 3 washing steps, antibody signals were amplified with the VectaStain ABC-Kit (Vector Laboratories) for 60 min at room temperature. After the slides had been rinsed with tris-buffered saline, they were incubated in nickel/diaminobenzidine solution for visualization of ABCB1 or A $\beta$ . The slides were washed, dehydrated, and mounted with Entellan (EMD Millipore). For the semiquantitative evaluation of ABCB1 in stained microvessels or A $\beta$  plaques in the hippocampus, cortex, or cerebellum, 4 visual fields ( $\times 20$ ) per mouse (4 animals per group) were counted and the mean of each group was calculated.

### Metabolism

In separate groups of wild-type and APP/PS1-21 mice, different tissues and fluids were analyzed with radio-thin-layer chromatography for radiolabeled metabolites of <sup>11</sup>C-metoclopramide at 15 min after radiotracer injection.

Female wild-type mice ( $n = 4$ ) and APP/PS1-21 mice ( $n = 6$ ) aged approximately 170 days were intraperitoneally treated for 7 days once daily with either PCN (25 mg/kg) or its vehicle (5% dimethylsulfoxide in safflower oil). On the day following the last treatment, animals were injected via the tail vein under isoflurane/air anesthesia with <sup>11</sup>C-metoclopramide ( $15 \pm 12$  MBq mixed with unlabeled metoclopramide, 2 mg/kg). After 15 min, a terminal blood sample was collected from the retrobulbar plexus and the animals were killed by cervical dislocation while under deep anesthesia. Brain, liver, kidneys, and gallbladder were removed, and urine was collected. Blood was centrifuged to obtain plasma, and proteins were precipitated by the addition of acetonitrile (1  $\mu$ L per  $\mu$ L of plasma). After homogenization of brain, liver, and kidney tissue, acetonitrile was added to precipitate proteins (1,000  $\mu$ L per liver, 200  $\mu$ L per brain/kidneys). Urine and bile were diluted by addition of acetonitrile (1  $\mu$ L per 2  $\mu$ L of urine, 2  $\mu$ L per  $\mu$ L of bile). All solutions were stirred in a vortex mixer and then centrifuged (12,000g, 1 min, 21°C). Each supernatant (plasma, brain, liver, bile, kidneys, and urine; 5  $\mu$ L each), and diluted <sup>11</sup>C-metoclopramide solution as a reference, were spotted on thin-layer chromatography plates (silica gel 60F 254 nm, 10  $\times$  20 cm; Merck), which were developed in ethyl acetate/ethanol/ammonium hydroxide (25%, w/v) (80/20/5, v/v/v). Detection was performed by placing the thin-layer chromatography plates on multisensitive phosphor screens (Perkin-Elmer Life Sciences). The screens were scanned at a 300-dpi resolution using a Cyclone Plus Phosphor Imager (Perkin-Elmer Life Sciences). The R<sub>f</sub> for <sup>11</sup>C-metoclopramide was 0.45, whereas the radiolabeled metabolites remained at the start (R<sub>f</sub> = 0).

### PET Data Analysis

The PET data were sorted into 25 time frames with a duration increasing from 5 s to 20 min. PET images were reconstructed using Fourier rebinning of the 3-dimensional sinograms followed by a 2-dimensional filtered backprojection with a ramp filter, giving a voxel size of 0.4  $\times$  0.4  $\times$  0.796 mm. Using PMOD software (version 3.6; PMOD Technologies Ltd.), hippocampus, cortex, and cerebellum

were outlined on the PET images using the Mirrione Mouse Atlas and guided by representative MR images obtained for a few animals on a 1-T benchtop MR scanner (ICON; Bruker BioSpin GmbH). Regions of interest were manually adjusted if necessary to derive time-activity curves expressed in units of SUV ([radioactivity per gram / injected radioactivity]  $\times$  body weight). From the log-transformed time-activity curves in hippocampus, cortex, and cerebellum, the elimination slope of radioactivity washout ( $k_{E,brain}$ , 1/h) was determined by linear regression analysis of data from 17.5 to 80 min after radiotracer injection (which best reflected the linear elimination phase in the log-transformed time-activity curves) (22,23).

### Statistical Analysis

Statistical testing was performed using Prism software (version 8.0; GraphPad). Differences between multiple groups were analyzed by 1-way ANOVA followed by a Tukey multiple-comparison test, and differences between 2 groups were analyzed by a 2-sided unpaired *t* test. The Pearson correlation coefficient (*r*) was calculated to assess correlations. The level of statistical significance was set to a *P* value of less than 0.05. All values are given as mean  $\pm$  SD.

## RESULTS

We used <sup>11</sup>C-metoclopramide PET to measure cerebral ABCB1 activity in groups of wild-type and APP/PS1-21 mice at baseline and after treatment with the ABCB1 inducer PCN (25 mg/kg) or its vehicle over 7 d. In Table 1, an overview of all examined mouse groups and corresponding animal numbers is given. Of the 65 animals, 20 died either during the treatment periods (8 animals) or during anesthesia (12 animals). PCN treatment resulted in 4 and 3 animal losses in the wild-type and APP/PS1-21 groups, respectively (PET and metabolism).

Treatment with neither PCN nor its vehicle led to significant changes in total radioactivity concentrations in blood or plasma measured at the end of the PET scan (Supplemental Fig. 1; supplemental materials are available at <http://jnm.snmjournals.org>). Analysis of radiolabeled metabolites of <sup>11</sup>C-metoclopramide at 15 min after radiotracer injection showed that approximately 60%–75% of total radioactivity in plasma comprised unidentified

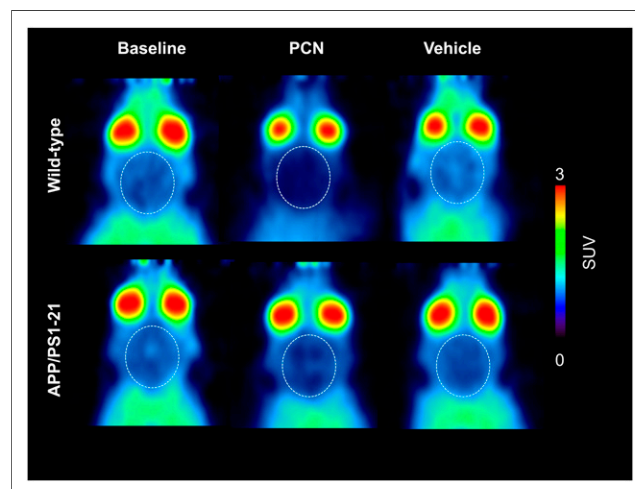


**FIGURE 1.** Coronal PET summation images (17.5–80 min) of wild-type and APP/PS1-21 mice aged 170 d for baseline scan and scan after intraperitoneal treatment with PCN or vehicle. Whole brain region is encircled with dashed line. All images are set to same intensity scale (0–3 SUV).

polar radiolabeled metabolites, whereas the majority (>80%) of radioactivity in the brain comprised unmetabolized  $^{11}\text{C}$ -metoclopramide (Supplemental Table 1). There was no significant difference in the percentage of unmetabolized  $^{11}\text{C}$ -metoclopramide in the brain between PCN-treated mice and vehicle-treated wild-type or APP/PS1-21 mice. In plasma, the percentage of unmetabolized  $^{11}\text{C}$ -metoclopramide was significantly lower in PCN-treated mice than in vehicle-treated wild-type mice.

In Figure 1, coronal  $^{11}\text{C}$ -metoclopramide PET summation images of wild-type and APP/PS1-21 mice at baseline and after treatment with PCN or vehicle are shown. For both mouse strains, PCN-treated animals had visually lower brain radioactivity concentrations. We outlined hippocampus and cortex as brain regions with substantial A $\beta$  deposition and cerebellum as a control region with minimal A $\beta$  deposition (Supplemental Fig. 2). In Figure 2, the time-activity curves for these regions are shown. In all 3 examined regions, PCN-treated wild-type and APP/PS1-21 mice showed a markedly increased washout of radioactivity as compared with the other groups (Fig. 2).

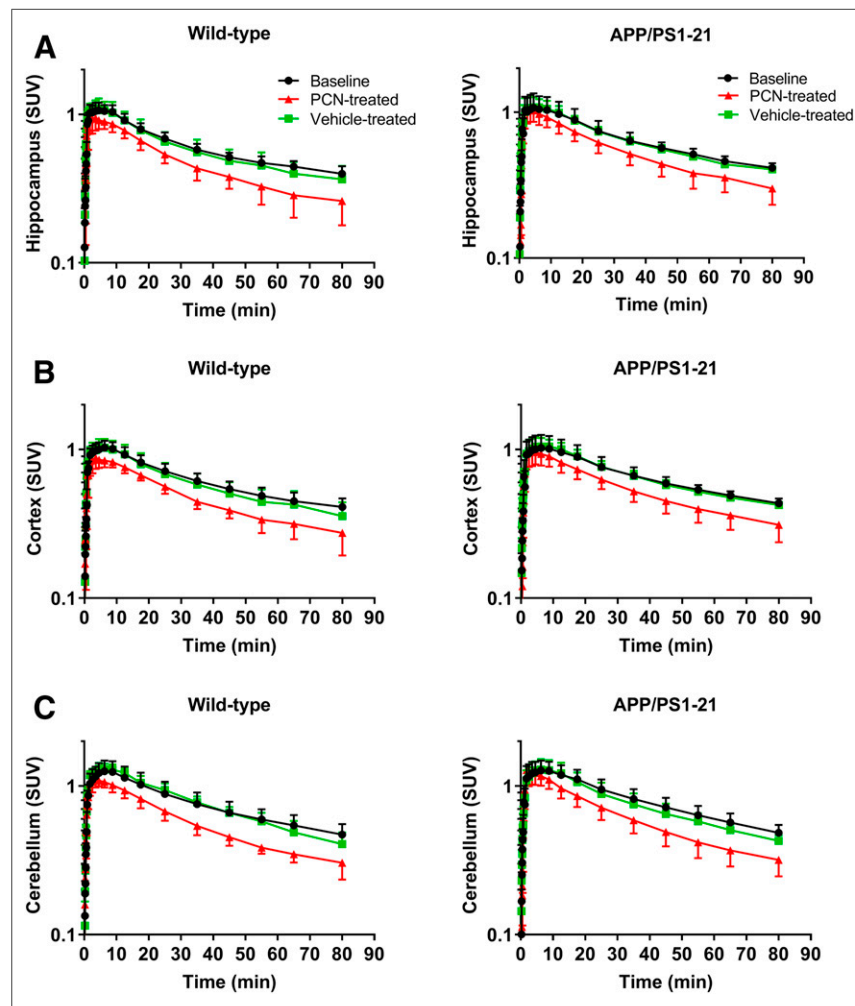
Brain slices of PCN- and vehicle-treated APP/PS1-21 mice were immunohistochemically stained for ABCB1 and A $\beta$  (Supplemental

Fig. 3). A semiquantitative analysis of the stained microvessels indicated significantly increased ABCB1 levels in the hippocampus, cortex, and cerebellum of PCN-treated compared with vehicle-treated APP/PS1-21 mice (Fig. 3A). In addition, a significant reduction in A $\beta$  plaque load was observed in the hippocampus and cortex of PCN-treated mice (Fig. 3A). There was a significant negative correlation between A $\beta$  plaque load and ABCB1 level in the hippocampus and a trend toward a negative correlation in the cortex (Fig. 3B). In the cerebellum, this correlation could not be assessed because of absence of A $\beta$  plaques.

As an outcome parameter of cerebral ABCB1 activity, we determined the  $k_{E,\text{brain}}$  from 17.5 to 80 min after radiotracer injection as described previously (22,23). Mean  $k_{E,\text{brain}}$  in all studied animal groups is given in Supplemental Table 2.  $k_{E,\text{brain}}$  was significantly increased in all 3 brain regions of PCN-treated wild-type and APP/PS1-21 mice (from +26% to +54% relative to the respective baseline group) (Fig. 4). There was a significant positive correlation between  $k_{E,\text{brain}}$  and ABCB1 level in the cortex and cerebellum of APP/PS1-21 mice and a trend toward a positive correlation in the hippocampus (Fig. 5).

We also performed baseline  $^{11}\text{C}$ -metoclopramide PET scans on

50-d-old wild-type and APP/PS1-21 mice to study possible age-related differences in cerebral ABCB1 activity. In all 3 brain regions of wild-type mice, there was a significant age-related decrease in  $k_{E,\text{brain}}$  (from -10% to -26%), whereas this effect was not observed in APP/PS1-21 mice (Fig. 6).  $k_{E,\text{brain}}$  did not differ significantly in any studied brain region between age-matched wild-type and APP/PS1-21 mice.



**FIGURE 2.** Mean ( $\pm$ SD) time-activity curves in wild-type mice and APP/PS1-21 mice aged 170 d for baseline PET scan and scan after intraperitoneal treatment with PCN or vehicle for hippocampus (A), cortex (B), and cerebellum (C).

## DISCUSSION

The aim of this study was to investigate whether the weak ABCB1 substrate radiotracer  $^{11}\text{C}$ -metoclopramide can measure ABCB1 induction at the mouse BBB. We found that treatment of wild-type and APP/PS1-21 mice with the prototypical rodent PXR ligand PCN led to significant increases in brain clearance of  $^{11}\text{C}$ -metoclopramide, as was consistent with ABCB1 induction. Moreover, the outcome parameter of  $^{11}\text{C}$ -metoclopramide elimination from the brain ( $k_{E,\text{brain}}$ ) was shown to be correlated with cerebral ABCB1 level, supporting the ability of  $^{11}\text{C}$ -metoclopramide to measure ABCB1 activity in the mouse brain and highlighting the potential of  $^{11}\text{C}$ -metoclopramide for future clinical translation to measure ABCB1 induction at the human BBB.

Currently available PET tracers for ABCB1 ( $^{11}\text{C}$ -verapamil, (*R*)- $^{11}\text{C}$ -verapamil, and  $^{11}\text{C}$ -*N*-desmethyl-loperamide) are efficiently transported by ABCB1 at the BBB, resulting in very low brain uptake and a limited sensitivity to measure moderate changes in ABCB1 activity at the BBB (18,19). Moreover, (*R*)- $^{11}\text{C}$ -verapamil is extensively metabolized in humans, giving rise to radiolabeled

metabolites that may be able to penetrate the BBB and thereby confound the measurement of ABCB1 activity (26). One study has so far attempted to measure ABCB1 induction at the human BBB with  $^{11}\text{C}$ -verapamil PET after treatment of healthy volunteers with the PXR activator rifampicin (27). That study failed to demonstrate an effect of rifampicin on cerebral ABCB1 activity, a finding that may be attributed either to the inability of rifampicin to induce ABCB1 at the human BBB or to the lack of sensitivity of  $^{11}\text{C}$ -verapamil to measure ABCB1 induction.

$^{11}\text{C}$ -metoclopramide was found to be, *in vitro*, a substrate of human ABCB1, although not being transported by breast cancer resistance protein (ABCG2), another major ABC transporter at the BBB (20). Moreover, chromatographic analysis of brain tissue homogenates obtained after intravenous injection of  $^{11}\text{C}$ -metoclopramide into rats demonstrated an absence of radiolabeled metabolites, suggesting that measurement of cerebral ABCB1 activity is not confounded by brain-penetrant radiolabeled metabolites (20). Finally, as opposed to avid ABCB1 substrates, pharmacologic inhibition of ABCB1 at the BBB was shown mainly to decrease the efflux rate constant of  $^{11}\text{C}$ -metoclopramide from the brain into the blood ( $k_2$ ), rather than increase the influx rate constant from plasma into the brain ( $K_1$ ) (19). Because the estimation of  $k_2$  requires a metabolite-corrected arterial input function,  $k_{E,\text{brain}}$  has been proposed as a parameter reflecting cerebral ABCB1 activity—a parameter that can be derived directly from the brain time-activity curves without the need to consider an arterial input function (22,23). A significant decrease in  $k_{E,\text{brain}}$  was found in nonhuman primates and healthy human volunteers after ABCB1 inhibition with tariquidar or

cyclosporine A (22,23). Considering that continuous arterial blood sampling is challenging in mice,  $k_{E,\text{brain}}$  was used in the present study as an outcome parameter of cerebral ABCB1 activity. We coinjected  $^{11}\text{C}$ -metoclopramide with unlabeled metoclopramide (2 mg/kg), because a previous study on rats had shown that this procedure slows the peripheral metabolism of the radiotracer while maintaining the ability of the radiotracer to measure cerebral ABCB1 activity (20). Nevertheless, substantial metabolism of  $^{11}\text{C}$ -metoclopramide was observed, with only 25%–40% of total radioactivity in plasma being in the form of unmetabolized radiotracer at 15 min after radiotracer injection (Supplemental Table 1). Importantly, in accordance with previous data on rats (20), we could demonstrate that most of the radioactivity in the mouse brain comprised unmetabolized  $^{11}\text{C}$ -metoclopramide. The fast plasma clearance of  $^{11}\text{C}$ -metoclopramide in mice may prove advantageous to the use of  $k_{E,\text{brain}}$  as a parameter of cerebral ABCB1 activity, as it suggests that  $k_{E,\text{brain}}$  will approximate the clearance of  $^{11}\text{C}$ -metoclopramide from brain into blood. However, validation would be required through arterial blood sampling and kinetic modeling to compare modeling-derived  $k_2$  values with  $k_{E,\text{brain}}$ .

We used a validated treatment protocol with the rodent PXR activator PCN to induce ABCB1 expression at the mouse BBB (9). PXR is a nuclear receptor that regulates the expression of metabolic enzymes and transporters involved in clearance of xenobiotics from the body. Hartz et al. have shown an increase in ABCB1 expression and activity and a concomitant decrease in  $\text{A}\beta$  level in isolated brain microvessels of 12-wk-old Tg2576 mice treated intraperitoneally over 7 d with PCN (25 mg/kg)

as compared with vehicle-treated animals (9). These previous findings could be confirmed in our study, in which the same PCN treatment protocol led to significant increases in ABCB1 level in all studied brain regions of APP/PS1-21 mice (Fig. 3). Moreover, a significant reduction in hippocampal and cortical  $\text{A}\beta$  levels was observed in PCN-treated mice, as was a negative correlation between  $\text{A}\beta$  and ABCB1 levels. A similar inverse correlation between  $\text{A}\beta$  and ABCB1 has been reported in brain tissue of nondemented elderly subjects (28). PCN treatment increased the percentage of radiolabeled metabolites of  $^{11}\text{C}$ -metoclopramide in plasma, as was consistent with the known CYP450 enzyme-inducing effect of PXR activation in the liver, but this increase had no effect on the composition of radioactivity in the brain (Supplemental Table 1). Baseline brain uptake of  $^{11}\text{C}$ -metoclopramide was higher than described previously in the same mouse strain for the avid ABCB1 substrates (*R*)- $^{11}\text{C}$ -verapamil and  $^{11}\text{C}$ -*N*-desmethyl-loperamide (29). Both in wild-type and in APP-PS1-21 mice, PCN treatment accelerated washout of radioactivity from the brain, as reflected by a significant increase in  $k_{E,\text{brain}}$  (Figs. 2 and 4). Moreover,  $k_{E,\text{brain}}$  in individual animals correlated positively with the respective cerebral ABCB1 levels (Fig. 5), thus corroborating the use of  $k_{E,\text{brain}}$  as an

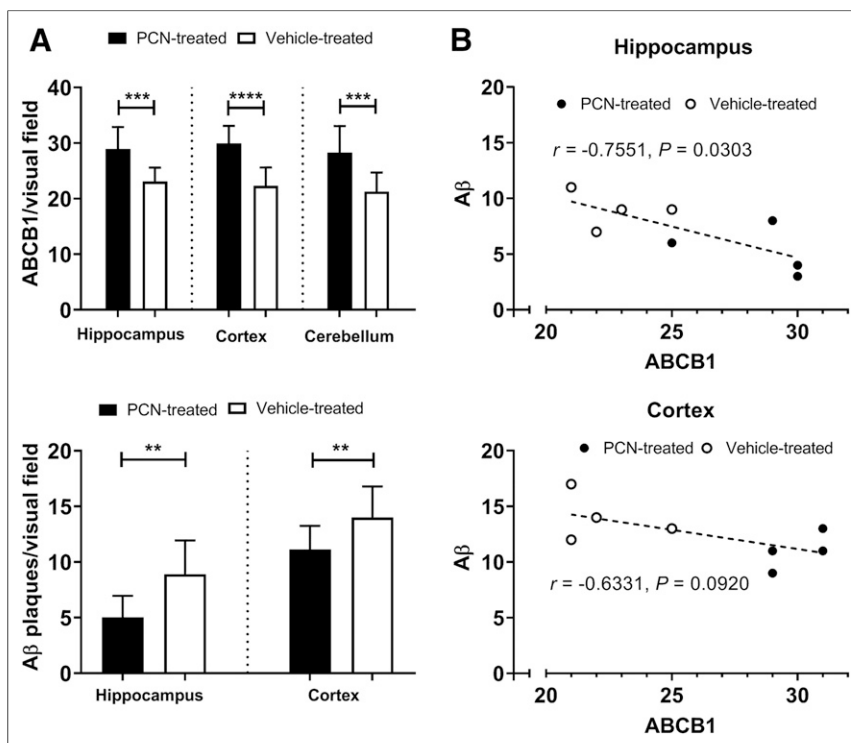


**FIGURE 3.** Semiquantitative evaluation of stained ABCB1 in microvessels and  $\text{A}\beta$  plaques in brains of APP/PS1-21 mice. (A) Four visual fields ( $\times 20$ ) per mouse ( $n = 4$ ) were counted, and mean of each group was calculated. Error bars indicate SD. (B) Correlations between  $\text{A}\beta$  and ABCB1 in hippocampus and in cortex are shown for data from APP/PS1-21 mice aged 170 d treated with PCN ( $n = 4$ ) or vehicle ( $n = 4$ ).  $r$  = Pearson correlation coefficient.  $**P < 0.01$ .  $***P < 0.001$ .  $****P < 0.0001$ .  $P$  values are for 2-sided unpaired  $t$  test.

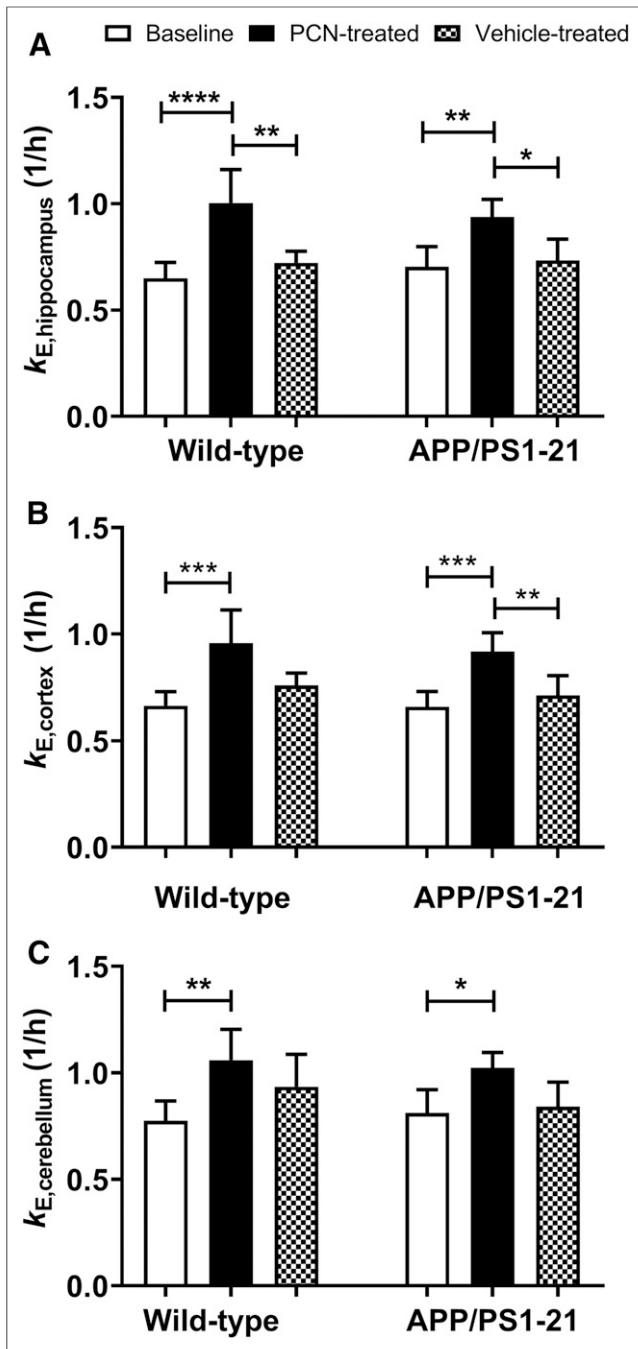


**FIGURE 4.**  $k_{E,brain}$  (mean  $\pm$  SD) for hippocampus (A), cortex (B), and cerebellum (C) in wild-type and APP/PS1-21 mice aged 170 d at baseline and after treatment with PCN or vehicle. \* $P < 0.05$ . \*\* $P < 0.01$ . \*\*\* $P < 0.001$ . \*\*\*\* $P < 0.0001$ .  $P$  values are for 1-way ANOVA followed by Tukey multiple-comparison test

outcome parameter for noninvasive determination of cerebral ABCB1 activity.

Accumulating evidence points to an age-related decline in cerebral ABCB1 expression and activity (30). In line with this evidence,  $k_{E,brain}$  was found to be significantly lower in all 3 brain regions of 170-d-old wild-type mice than in the 50-d-old group (Fig. 6). However, no statistically significant age-related decrease in  $k_{E,brain}$  was found in APP/PS1-21 mice. Moreover, no differences in  $k_{E,brain}$

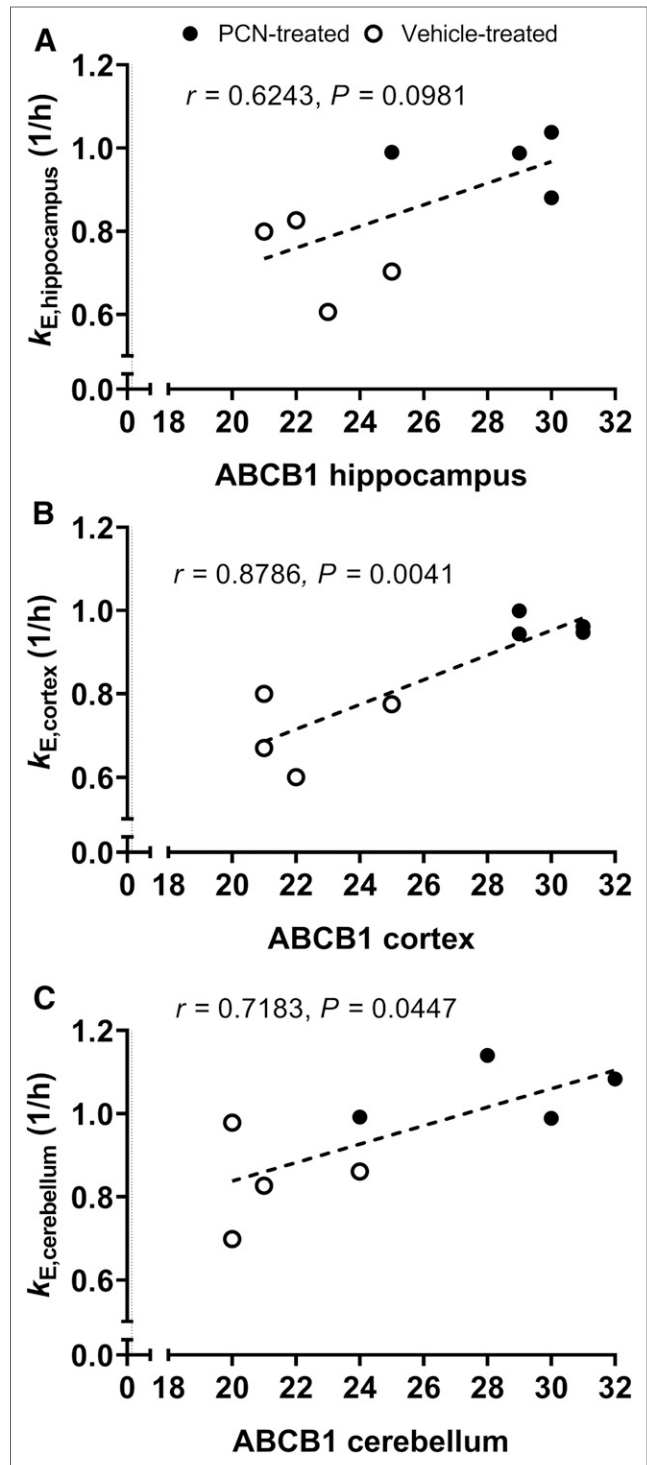


**FIGURE 5.** Correlations of  $k_{E,brain}$  with ABCB1 levels determined by immunohistochemistry in hippocampus (A), cortex (B), and cerebellum (C) of APP/PS1-21 mice aged 170 d treated with PCN ( $n = 4$ ) or vehicle ( $n = 4$ ).  $r$  = Pearson correlation coefficient.

were detected between age-matched wild-type and APP/PS1-21 mice. This result is surprising given that we previously found significantly reduced hippocampal and cortical ABCB1 levels in 200-d-old APP/PS1-21 mice as compared with age-matched wild-type mice (6). Thus, there is a possibility that additional alterations may have

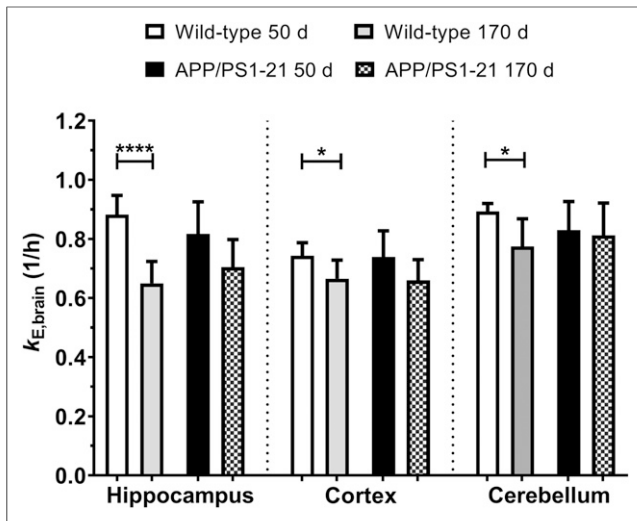


**FIGURE 6.**  $k_{E,brain}$  (mean  $\pm$  SD) for hippocampus, cortex, and cerebellum of wild-type and APP/PS1-21 mice aged 50 and 170 d at baseline. \* $P < 0.05$ . \*\*\*\* $P < 0.0001$ .  $P$  values are for 2-sided unpaired  $t$  test.

occurred at the BBB of APP/PS1-21 mice (e.g., decreases in cerebral blood flow, changes in structure or composition of the basement membrane) (7) and masked the impact of reduced ABCB1 expression on the brain kinetics of  $^{11}\text{C}$ -metoclopramide. A possible alternative explanation is that the lot of wild-type and APP/PS1-21 mice used in the present study—even though it was obtained from the same source as in our previous study (6)—showed no differences in cerebral ABCB1 levels. Such a possibility could not be confirmed because of a lack of immunohistochemical data for wild-type mice.

## CONCLUSION

Our data provide clear evidence for the suitability of  $^{11}\text{C}$ -metoclopramide, a novel weak ABCB1 substrate radiotracer, to measure ABCB1 induction at the mouse BBB without the need to consider an arterial input function.  $^{11}\text{C}$ -metoclopramide may overcome the limitations of previously described avid ABCB1 substrate radiotracers and provide an imaging-based biomarker for the development of novel ABCB1-inducing AD therapeutics. Next to measuring pharmacologic induction of cerebral ABCB1,  $^{11}\text{C}$ -metoclopramide PET may also be suitable to measure a disease-induced increase in cerebral ABCB1 activity (e.g., in drug-resistant epilepsy).

## DISCLOSURE

This work was supported by the Austrian Science Fund (FWF) (I 1609-B24, to Oliver Langer), the Deutsche Forschungsgemeinschaft (DFG) (DFG PA930/9-1, to Jens Pahnke), and the Lower Austria Corporation for Research and Education (NFB) (LS14-008, to Thomas Wanek). The work of Jens Pahnke was further supported by the following grants: Deutsche Forschungsgemeinschaft/Germany (DFG PA930/12), Wirtschaftsministerium Sachsen-Anhalt (EFRE, ZS/2016/05/78617), the Leibniz Association (Leibniz-Wettbewerb SAW-2015-IPB-2), Latvian Council of Science FLPP/Latvia (Izp-2018/1-0275), Nasjonalforeningen (16154), HelseSØ/Norway (2016062, 2019054, 2019055), Norsk forskningsrådet/Norway (251290 FRIMEDIO, 260786 PROP-AD), and Horizon 2020/European Union (643417, PROP-AD). PROP-AD is a European Union Joint Programme-Neurodegenerative Disease Research (JPND)

project. The project is supported through the following funding organizations under the aegis of JPND-www.jpnd.eu: AKA 301228-Finland, BMBF 01ED1605-Germany, CSO-MOH 30000-12631-Israel, NFR 260786-Norway, and SRC 2015-06795-Sweden. This project has received funding from the European Union's Horizon 2020 research and innovation program under grant agreement 643417 (JPco-fuND). No other potential conflict of interest relevant to this article was reported.

## ACKNOWLEDGMENTS

We thank Mathilde Löbsch for help in conducting the PET experiments.

## KEY POINTS

**QUESTION:** Can  $^{11}\text{C}$ -metoclopramide PET measure ABCB1 induction at the BBB?

**PERTINENT FINDINGS:** Treatment of wild-type and APP/PS1-21 mice with the prototypical rodent PXR activator PCN over 7 d led to a significant increase in  $k_{E,brain}$ . Immunohistochemical analysis confirmed ABCB1 induction in PCN-treated APP/PS1-21 mice and a concomitant reduction in A $\beta$  load.

**IMPLICATIONS FOR PATIENT CARE:**  $^{11}\text{C}$ -metoclopramide PET may aid in the future development of novel AD therapeutics that increase cerebral ABCB1 activity to enhance clearance of neurotoxic A $\beta$  peptides from the brain.

## REFERENCES

- Boland B, Yu WH, Corti O, et al. Promoting the clearance of neurotoxic proteins in neurodegenerative disorders of ageing. *Nat Rev Drug Discov*. 2018;17:660–688.
- Mawuenyega KG, Sigurdson W, Ovod V, et al. Decreased clearance of CNS beta-amyloid in Alzheimer's disease. *Science*. 2010;330:1774.
- Hardy J, Allsop D. Amyloid deposition as the central event in the aetiology of Alzheimer's disease. *Trends Pharmacol Sci*. 1991;12:383–388.
- Abbott NJ, Patabendige AA, Dolman DE, Yusof SR, Begley DJ. Structure and function of the blood-brain barrier. *Neurobiol Dis*. 2010;37:13–25.
- Storck SE, Hartz AMS, Bernard J, et al. The concerted amyloid-beta clearance of LRP1 and ABCB1/P-gp across the blood-brain barrier is linked by PICALM. *Brain Behav Immun*. 2018;73:21–33.
- Zoufal V, Wanek T, Krohn M, et al. Age dependency of cerebral P-glycoprotein function in wild-type and APPS1 mice measured with PET. *J Cereb Blood Flow Metab*. 2020;40:150–162.
- Mehta DC, Short JL, Nicolazzo JA. Altered brain uptake of therapeutics in a triple transgenic mouse model of Alzheimer's disease. *Pharm Res*. 2013;30:2868–2879.
- Kannan P, Schain M, Kretzschmar WW, et al. An automated method measures variability in P-glycoprotein and ABCG2 densities across brain regions and brain matter. *J Cereb Blood Flow Metab*. 2017;37:2062–2075.
- Hartz AM, Miller DS, Bauer B. Restoring blood-brain barrier P-glycoprotein reduces brain amyloid-beta in a mouse model of Alzheimer's disease. *Mol Pharmacol*. 2010;77:715–723.
- Deo AK, Borson S, Link JM, et al. Activity of P-glycoprotein, a beta-amyloid transporter at the blood-brain barrier, is compromised in patients with mild Alzheimer disease. *J Nucl Med*. 2014;55:1106–1111.
- Miller DS. Regulation of ABC transporters blood-brain barrier: the good, the bad, and the ugly. *Adv Cancer Res*. 2015;125:43–70.
- Qosa H, Abuznait AH, Hill RA, Kaddoumi A. Enhanced brain amyloid-beta clearance by rifampicin and caffeine as a possible protective mechanism against Alzheimer's disease. *J Alzheimers Dis*. 2012;31:151–165.
- Brenn A, Grube M, Jedlitschky G, et al. St. John's wort reduces beta-amyloid accumulation in a double transgenic Alzheimer's disease mouse model: role of P-glycoprotein. *Brain Pathol*. 2014;24:18–24.
- Durk MR, Han K, Chow EC, et al.  $1\alpha,25$ -dihydroxyvitamin  $\text{D}_3$  reduces cerebral amyloid-beta accumulation and improves cognition in mouse models of Alzheimer's disease. *J Neurosci*. 2014;34:7091–7101.

15. Muzi M, Mankoff DA, Link JM, et al. Imaging of cyclosporine inhibition of P-glycoprotein activity using <sup>11</sup>C-verapamil in the brain: studies of healthy humans. *J Nucl Med.* 2009;50:1267–1275.
16. Kreisl WC, Bhatia R, Morse CL, et al. Increased permeability-glycoprotein inhibition at the human blood-brain barrier can be safely achieved by performing PET during peak plasma concentrations of tariquidar. *J Nucl Med.* 2015;56:82–87.
17. Bauer M, Karch R, Zeitlinger M, et al. Approaching complete inhibition of P-glycoprotein at the human blood-brain barrier: an (R)-[<sup>11</sup>C]verapamil PET study. *J Cereb Blood Flow Metab.* 2015;35:743–746.
18. Tournier N, Stieger B, Langer O. Imaging techniques to study drug transporter function in vivo. *Pharmacol Ther.* 2018;189:104–122.
19. Bauer M, Tournier N, Langer O. Imaging P-glycoprotein function at the blood-brain barrier as a determinant of the variability in response to central nervous system drugs. *Clin Pharmacol Ther.* 2019;105:1061–1064.
20. Pottier G, Marie S, Goutal S, et al. Imaging the impact of the P-glycoprotein (ABCB1) function on the brain kinetics of metoclopramide. *J Nucl Med.* 2016; 57:309–314.
21. Savolainen H, Windhorst AD, Elsinga PH, et al. Evaluation of [<sup>18</sup>F]MC225 as a PET radiotracer for measuring P-glycoprotein function at the blood-brain barrier in rats: kinetics, metabolism, and selectivity. *J Cereb Blood Flow Metab.* 2017;37:1286–1298.
22. Tournier N, Bauer M, Pichler V, et al. Impact of P-glycoprotein function on the brain kinetics of the weak substrate <sup>11</sup>C-metoclopramide assessed with PET imaging in humans. *J Nucl Med.* 2019;60:985–991.
23. Auvity S, Caillé F, Marie S, et al. P-glycoprotein (ABCB1) inhibits the influx and increases the efflux of <sup>11</sup>C-metoclopramide across the blood-brain barrier: a PET study on non-human primates. *J Nucl Med.* 2018;59:1609–1615.
24. Radde R, Bolmont T, Kaeser SA, et al. Aβ<sub>42</sub>-driven cerebral amyloidosis in transgenic mice reveals early and robust pathology. *EMBO Rep.* 2006;7:940–946.
25. Caillé F, Goutal S, Marie S, et al. Positron emission tomography imaging reveals an importance of saturable liver uptake transport for the pharmacokinetics of metoclopramide. *Contrast Media Mol Imaging.* 2018;2018:7310146.
26. Luurtsema G, Molthoff CF, Schuit RC, Windhorst AD, Lammertsma AA, Franssen EJ. Evaluation of (R)-[<sup>11</sup>C]verapamil as PET tracer of P-glycoprotein function in the blood-brain barrier: kinetics and metabolism in the rat. *Nucl Med Biol.* 2005;32:87–93.
27. Liu L, Collier AC, Link JM, et al. Modulation of P-glycoprotein at the human blood-brain barrier by quinidine or rifampin treatment: a PET imaging study. *Drug Metab Dispos.* 2015;43:1795–1804.
28. Vogelgesang S, Cascorbi I, Schroeder E, et al. Deposition of Alzheimer's beta-amyloid is inversely correlated with P-glycoprotein expression in the brains of elderly non-demented humans. *Pharmacogenetics.* 2002;12:535–541.
29. Wanek T, Römermann K, Mairinger S, et al. Factors governing p-glycoprotein-mediated drug-drug interactions at the blood-brain barrier measured with positron emission tomography. *Mol Pharm.* 2015;12:3214–3225.
30. Pan Y, Nicolazzo JA. Impact of aging, Alzheimer's disease and Parkinson's disease on the blood-brain barrier transport of therapeutics. *Adv Drug Deliv Rev.* 2018;135:62–74.